




RNA activation-independent DNA targeting of the Type III CRISPR-Cas system by a Csm complex

Kwang-Hyun Park¹, Yan An¹, Tae-Yang Jung^{2,3,4}, In-Young Baek¹, Haemin Noh², Woo-Chan Ahn^{1,2} , Hans Hebert^{3,4}, Ji-Joon Song² , Jeong-Hoon Kim⁵, Byung-Ha Oh^{2,*} & Eui-Jeon Woo^{1,6,**} 

Abstract

The CRISPR-Cas system is an adaptive and heritable immune response that destroys invading foreign nucleic acids. The effector complex of the Type III CRISPR-Cas system targets RNA and DNA in a transcription-coupled manner, but the exact mechanism of DNA targeting by this complex remains elusive. In this study, an effector Csm holocomplex derived from *Thermococcus onnurineus* is reconstituted with a minimalistic combination of Csm1₁2₁3₃4₁5₁, and shows RNA targeting and RNA-activated single-stranded DNA (ssDNA) targeting activities. Unexpectedly, in the absence of an RNA transcript, it cleaves ssDNA containing a sequence complementary to the bound crRNA guide region in a manner dependent on the HD domain of the Csm1 subunit. This nuclease activity is blocked by a repeat tag found in the host CRISPR loci. The specific cleavage of ssDNA without a target RNA suggests a novel ssDNA targeting mechanism of the Type III system, which could facilitate the efficient and complete degradation of foreign nucleic acids.

Keywords CRISPR; Csm complex; DNase; RNase; *Thermococcus onnurineus*

Subject Categories Microbiology, Virology & Host Pathogen Interaction; RNA Biology

DOI 10.15252/embr.201643700 | Received 20 November 2016 | Revised 19 February 2017 | Accepted 23 February 2017 | Published online 31 March 2017

EMBO Reports (2017) 18: 826–840

Introduction

Clustered regularly interspaced short palindromic repeats (CRISPR) and CRISPR-associated (Cas) systems eliminate invading phages and plasmids in prokaryotes [1–4]. CRISPR loci are composed of variable spacer sequences derived from genetic invaders and a series of short repeat sequences [4,5]. Transcripts from CRISPR loci are processed to generate short RNAs, termed crRNAs, that assemble with Cas proteins into a large nuclease effector complex [6].

Based on the *cas* gene content and the mechanism of action, CRISPR-Cas systems are classified into six major types (types I–VI) and at least 16 subtypes [7]. The multi-protein Cascade complex of the Type I system detects foreign nucleic acids and then recruits the Cas3 protein to degrade DNA using its HD nuclease domain [8,9]. Type II/V systems also target DNA, but recognition and cleavage are mediated by a ribonucleoprotein effector containing a single protein, Cas9 or Cpf1 [10–12]. The Cascade complex of Type I and the Csm and/or Cmr effector complexes of Type III are phylogenetically related multi-subunit ribonucleoprotein complexes, and in the holocomplex assembly, both form a common twisted helical structure with homologous components [13–16]. In contrast, the Type I and Type II systems target exclusively DNA, and the Type III system targets RNA or/and DNA [3,17–22].

The Type III system can be further classified into subtypes (subtypes III-A–III-D) or mainly into Type III-A and Type III-B [14,23]. The Csm complexes of Type III-A from *Sulfolobus solfataricus*, *Thermus thermophilus*, *Streptococcus thermophilus*, *Staphylococcus aureus* and *Staphylococcus epidermidis* have been characterized *in vitro* and *in vivo* [3,19,21–24]. The Csm complex consists of five subunits (Csm1–5) and a crRNA, while the Cmr complex of Type III-B consists of six subunits (Cmr1–6) and a crRNA [22,25,26]. The crRNA is composed of eight nucleotides (nt) at its 5' end, termed the 5' handle, and 30–45 nt, termed the guide sequence, derived from a spacer sequence of CRISPR. The common tag at the 5' end of the crRNA derived from the repeat sequence of the CRISPR is processed by Cas6 and recognized by the Csm4 or Cmr3 subunit in the complexes [27,28]. The Csm/Cmr complexes possess an RNase activity that cleaves target RNAs at the complementary guide region of crRNA at 6-nt intervals by means of multiple copies of Csm3 in the Csm complex [21,22] or Cmr4 in the Cmr complex [29].

The DNA targeting mechanism of the Type III system is a recent topic of ongoing investigation [30–32]. The target cleavage by the Type III-A system requires directional transcription that accompanies the displacement of the target double-stranded DNA (dsDNA) and the production of RNA transcripts [33]. The Csm complex from

1 Disease Target Structure Research Center, Korea Research Institute of Bioscience and Biotechnology, Daejeon, South Korea

2 Department of Biological Sciences, Korea Advanced Institute of Science and Technology (KAIST) Institute for the BioCentury, Daejeon, South Korea

3 Department of Biosciences and Nutrition, Karolinska Institute, Huddinge, Sweden

4 School of Technology and Health, KTH Royal Institute of Technology, Huddinge, Sweden

5 Personalized Genomic Medicine Research Center, Korea Research Institute of Bioscience and Biotechnology, Daejeon, South Korea

6 Department of Analytical Bioscience, University of Science and Technology, Daejeon, South Korea

*Corresponding author. Tel: +82 423502648; E-mail: bhoh@kaist.ac.kr

**Corresponding author. Tel: +82 428798432; E-mail: ejwoo@kribb.re.kr

S. epidermis degrades the RNA transcripts and the non-template DNA strand through the transcription-coupled targeting mechanism *in vitro* and *in vivo* by the nuclease activity of the Csm1 subunit [19]. The Csm complex from *S. thermophilus* exhibits a similar non-specific degradation of DNA in an RNA transcript-dependent manner with the catalytic site in the HD domain of Csm1 [30]. The Cmr complexes from *P. furiosus* and *T. maritima* cleave DNA and protect cells from plasmid invasion in a transcription-coupled manner by the HD domain of the Cmr2 subunit [22,32]. For the Type I and Type II systems, the protospacer adjacent motif (PAM) sequence plays a key role in discriminating between self and non-self DNA to recognize foreign nucleotides and facilitates the unwinding of the target DNA. Type III systems are unique in that they lack a PAM motif [13,34–36]. Instead of recognizing a distinct PAM sequence, the Csm complexes in Type III systems might check for complementarity between the repeat-derived region of the crRNA and the target DNA strand [37]. However, the exact mechanisms of the DNA targeting in Type III systems remain elusive, particularly those mechanisms underlying the positioning of the effector complex with respect to the separated ssDNA strands during transcription and the conformational change for the activation of nuclease activity.

In this study, we reconstituted the Csm effector holocomplex of *Thermococcus onnurineus* NA1 and found that this effector complex has a novel single-stranded DNA (ssDNA)-specific nuclease activity in addition to the previously known RNA targeting and RNA-activated DNA targeting activities. We report the characterization of this nuclease activity, designated as the RNA transcript-independent ssDNA targeting, which could ensure the direct recognition and degradation of the non-template strand of foreign DNA without affecting self DNA.

Results

In vitro assembly of the ToCsm complex

The hyperthermophilic archaeon, *T. onnurineus* NA1, has six CRISPR loci and two Cas systems, Type III-A and putative Type IV, according to a CRISPR database (Fig EV1A and B) [38,39]. The Type III-A-specific *csm* gene cluster (*Ton_0892–Ton_0898*) is located between CRISPR locus 3 and locus 4 (Fig 1A). We sought to reconstitute the effector holocomplex (ToCsm complex) composed of five different subunits (ToCsm1–ToCsm5) and a crRNA. We found that

the ToCsm1–Csm4 and ToCsm2–Csm5 subcomplexes could be produced in a soluble form in *E. coli* by coexpression of the respective subunits, while each individual subunit was insoluble. In contrast, ToCsm3 alone exhibited reasonable solubility. Incubation of these recombinant subcomplexes and the protein did not result in the formation of the ToCsm holocomplex. Subsequently, we synthesized crRNAs that contain a common 8-nt repeat sequence [27,37] at CRISPR locus 3, 5'-GUGGAAAG-3', and a spacer sequence with varying length ranging from 30 to 40 nt. Each of these crRNAs was incubated with purified ToCsm1–Csm4, ToCsm2–Csm5 and ToCsm3 at 60°C for 20 min. The mixtures showed a major single peak corresponding to an approximately 280 kDa mass in size-exclusion chromatography (SEC), indicating holocomplex assembly in the presence of a crRNA (Figs 1B and EV1C). Among the crRNAs, a 38-nt crRNA yielded the most significant peak in the SEC analysis and was thus selected for further functional studies. This peak fraction contained all five subunits of the ToCsm complex as shown by denaturing SDS polyacrylamide gel electrophoresis (PAGE) and displayed a single band on a native polyacrylamide gel. This fraction also contained the crRNA as identified by denaturing urea-PAGE (Fig 1C). A multi-angle light scattering (MALS) analysis indicated that this fraction corresponds to a molecular mass of 273.4 ($\pm 1.32\%$) kDa, which is consistent with the SEC analysis (Fig 1D). These data demonstrated that the ToCsm complex could be reconstituted *in vitro* in a stable, highly pure form with the recombinant components and the 38-nt crRNA.

To determine the overall structure of the complex, we performed single-particle electron microscopy (EM) for three-dimensional reconstruction. We recorded 24 images and extracted 7,644 individual particles (Fig EV2A). Reference-free 2D image classification allowed an initial appreciation of an elongated-helical shape of the complex with the longest dimension of 160 Å (Fig EV2B). The projections of the initial model map agreed well with the corresponding 2D averages. The three-dimensional reconstruction of the ToCsm complex revealed elongated and twisted blobs with dimensions of 160 × 90 × 90 Å. The final resolution of the maps was ~25 Å, calculated at 0.5 Fourier shell correlation (three sigma) (Fig EV2C). The crystal structure of the Cmr complex lacking the Cmr1 subunit (PDB ID: 3X1L) agrees well with the EM density of the ToCsm complex (Fig EV2D) [28]. Based on the position of Cmr2, which corresponds to Csm1, the crystal structure of ToCsm1 was fitted into the EM map, which positioned its HD domain at the bottom of the protruding lobe (Fig 1E). The complex was significantly smaller than that of *S. solfataricus* or *T. thermophilus* [16,22]

Figure 1. *In vitro* assembly of the ToCsm complex.

- A Organization of the *cas* locus of the Type III-A system in *T. onnurineus*. The ORFs between CRISPR loci 3 and 4 are shown. Blue arrows represent the *csm* genes encoding the ToCsm complex.
- B Size-exclusion chromatography. The elution profile of the ToCsm complex is presented with the deduced molecular weight (280 kDa). The size markers are thyroglobulin (669 kDa), ferritin (440 kDa), aldolase (158 kDa) and conalbumin (75 kDa).
- C SDS-PAGE, blue native (BN)-PAGE and urea-PAGE analyses.
- D Multi-angle light scattering (MALS) analysis of the ToCsm complex. SEC combined with MALS allowed the calculation of the molecular weight (Mw) distributions (dotted black line).
- E Docking of the ToCsm1 structure (PDB ID: 4UW2) into the EM map of the ToCsm complex (EMD-3454). The HD domain of the ToCsm1 monomer is coloured blue (see Fig EV2D for the docking of the Cmr complex).
- F Comparison of the EM structures of the Csm complexes. Lengths and widths of the Csm complexes are shown.
- G Schematic representation of the ToCsm complex bound to crRNA. The active sites of the HD domain of the ToCsm1 (dotted circle) and the crRNA (grey line) are highlighted.

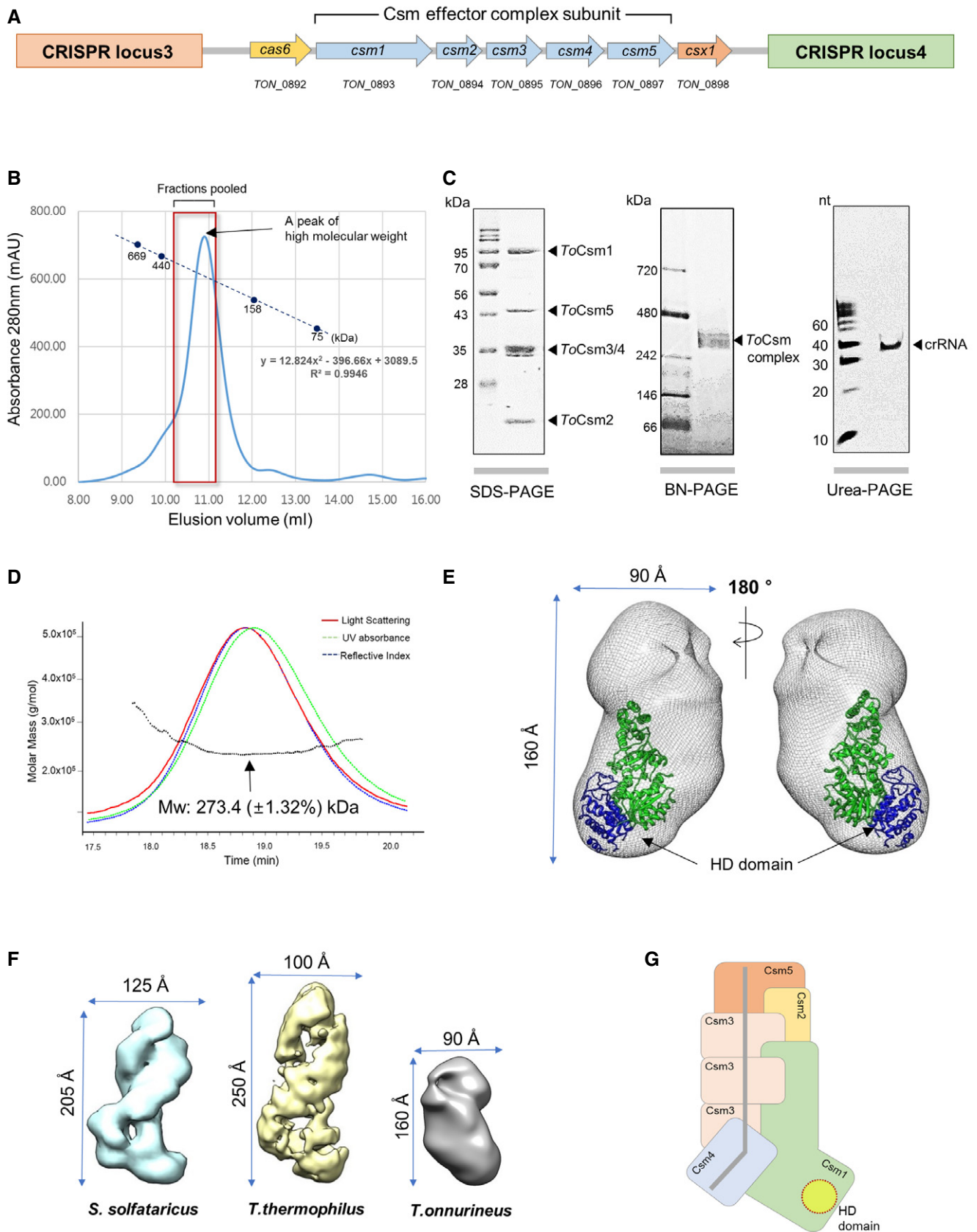


Figure 1.

(Fig 1F). The stoichiometry of the *ToCsm* complex was estimated as $1_1 2_1 3_3 4_1 5_1$ based on the EM density fitting and the molecular mass of each component. This is the smallest Csm complex reported to date (Fig 1G). In this complex, three copies of *ToCsm3* are likely to form the backbone to shape the twisted helical geometry, as similarly observed in the previously determined structures of the Csm and Cmr complexes [22,28].

RNase activity of the *ToCsm* complex

Csm complexes bind and cleave RNA transcripts that contain a sequence complementary to the guide region of the bound crRNA (termed the target sequence) [21,22]. To examine the RNA targeting activity of the *ToCsm* complex, we first synthesized a 40-nt RNA substrate containing a middle 30-nt target sequence and a 5-nt non-complementary sequence at both ends with a radio-label at the 5' end. This ssRNA substrate, termed target RNA, was incubated with the effector complex, and the reaction mixture was analysed in a time course on a denaturing gel. Three major cleaved products were observed that differ from each other by 6 or 12 nt: 30-, 24- and 18-nt RNA fragments (Figs 2A and EV3A). The cleavage pattern suggested that the target 40-nt RNA is cleaved predominantly at site 2 or 3. In accordance with previous studies, the *ToCsm* complex could not cleave an RNA substrate containing a non-complementary 30-nt sequence, termed non-target RNA, under the same reaction conditions, indicating that the sequence complementarity between the target RNA and the crRNA is essential for target RNA cleavage (Fig EV3B). This is consistent with the properties of the Csm complexes from *S. epidermidis*, *S. thermophilus* and *T. thermophilus* [19,21,22]. Previously, Csm3 was identified as the catalytic subunit responsible for the endoribonuclease activity of the Type III-A system in *S. thermophilus* [21]. We generated an active-site mutant of *ToCsm3* containing a D36A substitution (*ToCsm3*^{D36A}) and examined its effect on the RNase activity. The *Csm3*^{D36A} mutant did not affect the assembly of *ToCsm* but abolished the RNA cleavage activity of the effector complex. (Fig EV3C). These data show that the *ToCsm* complex shared the same backbone-mediated RNA cleavage activity as observed with other Type III effector complexes. Next, to examine whether the RNase activity might be affected by mutations in the *ToCsm1* subunit, which are known to abolish the RNA-coupled DNase activity, we produced *ToCsm* complexes reconstituted with a *ToCsm1* mutant, containing H14A/D15N double substitutions in its HD domain (*ToCsm1*^{H14A/D15N}, HD_m), D587A/D588A double substitutions in its GGDD motif (*ToCsm1*^{D587A/D588A}, DD_m) or H14A/D15N/D587A/D588A quadruple substitutions (*ToCsm1*^{H14A/D15N/D587A/D588A}, HD/DD_m). All three *ToCsm1* mutant-containing *ToCsm* complexes cleaved the target RNA without a notable difference compared with the wild-type *ToCsm* complex, demonstrating that these mutations affecting the DNA targeting activity of *ToCsm1* do not affect the RNA cleavage activity of the effector complex (Fig EV3D).

Target RNA-activated DNase activity of the *ToCsm* complex

We previously reported that the *ToCsm1* subunit alone degraded single-stranded DNA (ssDNA) non-specifically [40]. However, when the *ToCsm1* subunit was assembled in the *ToCsm* complex, its nuclease function was inhibited, and the complex could not degrade

non-specific ssDNA substrate. Recently, the Csm complex from *S. thermophilus* and the Cmr complex from *T. maritima* or *P. furiosus* were reported to degrade ssDNA only in the presence of a complementary RNA transcript [30–32]. To test whether the target RNA reactivates the DNase activity of the *ToCsm* complex, we prepared 5' radio-labelled linear 100-nt ssDNA substrates containing a sequence either complementary or non-complimentary to the bound crRNA, termed target ssDNA and non-target ssDNA, respectively. First, the *ToCsm* complex was pre-incubated with the synthesized 40-nt RNA, the same substrate used for the RNA cleavage assay, in the absence of any divalent metal ions. Then, the ssDNA substrate was added to the pre-incubated *ToCsm* complex in the presence of Ni²⁺ ion, a known metal cofactor for the nuclease activity of *ToCsm1* [40]. The *ToCsm* complex degraded the ssDNA substrates containing either the complementary sequence or the non-complementary sequence. The *ToCsm* complex containing *ToCsm1* (HD_m) or *ToCsm1* (HD_m/DD_m) did not show any cleavage activity towards the ssDNA substrate, whereas the *ToCsm* complex containing *ToCsm1* (DD_m) degraded the substrate in the presence of the 40-nt target RNA (Fig 2B). In comparison, the *ToCsm* complex did not degrade dsDNA substrates at all, regardless of the presence of a complementary sequence (Fig EV3E). To examine whether this DNase activity could be affected by the active site mutation (D36A) on the *ToCsm3* subunit that abolishes its RNA cleavage activity, we reconstituted the *ToCsm* complex containing *ToCsm3*^{D36A} and measured the DNase activity. The resulting mutant *ToCsm* complex cleaved the ssDNA substrate without a notable difference from the wild-type complex, indicating that the RNase activity of the *ToCsm3* subunit did not affect the DNA cleavage activity of the *ToCsm* complex (Fig EV3F). Together, these results demonstrate that the active site located at the HD domain of the *ToCsm1* subunit exhibits target RNA-activated nuclease activity towards ssDNA but not towards dsDNA. This non-sequence-specific DNase activity in the presence of the target RNA would completely degrade the ssDNA substrate.

Target RNA-independent binding of ssDNA via crRNA

In the target RNA-activated DNase assay, we noted that the *ToCsm* complex limitedly degraded linear ssDNA substrate containing a target sequence, producing a large uncleaved fragment (Fig 2B). In contrast, the complex degraded ssDNA substrate without a target sequence into much smaller fragments. An observation of the different cleavages of the two substrates led us to examine whether, in the absence of a target RNA, the *ToCsm* complex may directly target ssDNA substrate containing the complementary sequence. We synthesized 5' radio-labelled linear ssDNA, RNA and dsDNA, each containing a 30-nt complementary sequence inserted in the centre, and analysed their binding to the *ToCsm* complex by an electrophoretic mobility shift assay (EMSA). To avoid degradation by metal-dependent DNase or RNase activity, a metal chelator was added to the reaction buffer. The *ToCsm* complex significantly shifted the target ssDNA, indicating a direct binding unaided by a target RNA. This is in a sharp contrast with *ToCsm1*-Csm4, *ToCsm2*-Csm5 subcomplexes and *ToCsm3* protein, which did not result in a mobility shift of these nucleic acids (Fig EV4A and B). The dsDNA does not appear to interact with the *ToCsm* complex, as no shift was observed regardless of the presence or absence of

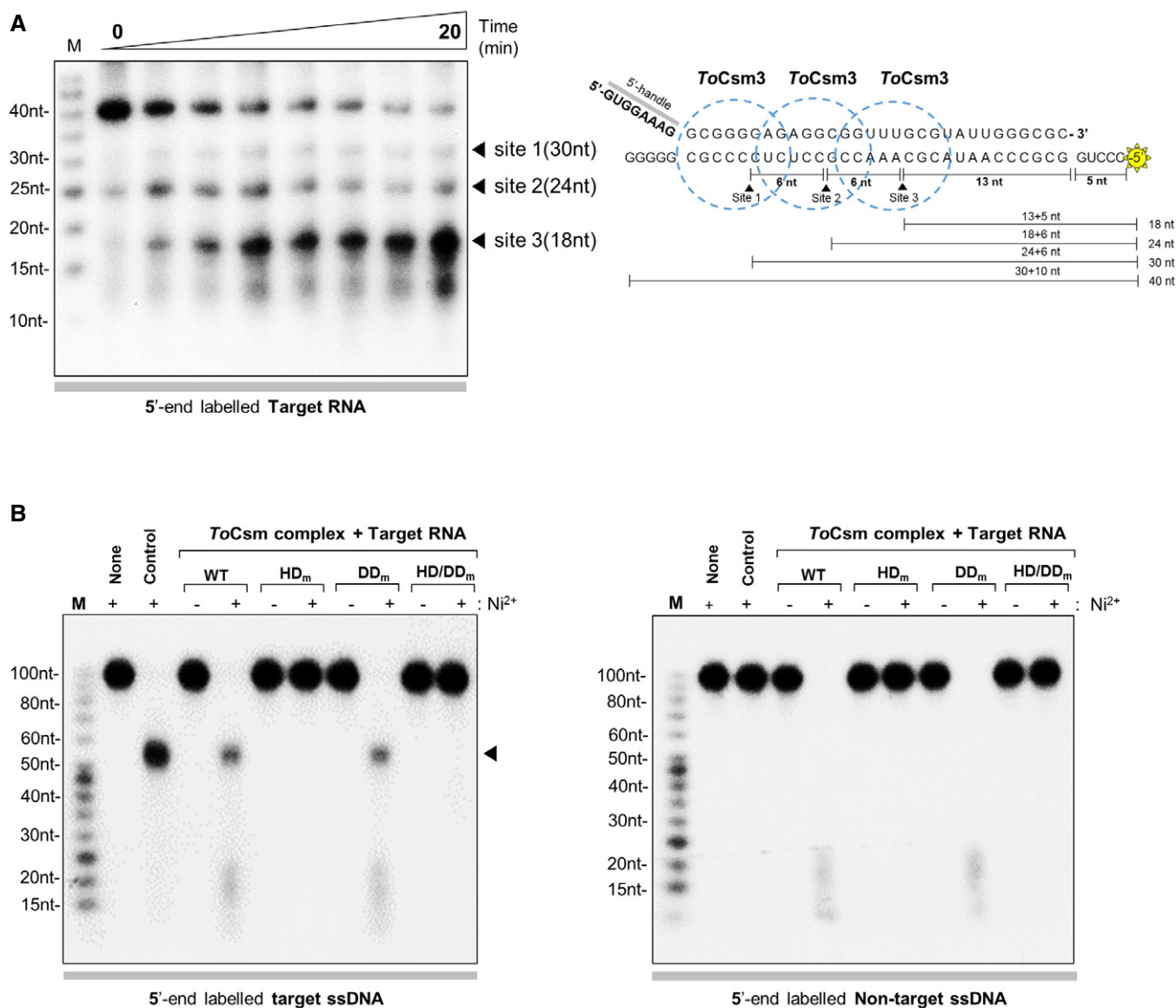


Figure 2. RNase activity and target RNA-activated ssDNase activity.

A Cleavage of 40-nt target RNA by the *ToCsm* complex in a time course (0, 0.5, 1, 3, 5, 10, 15, 20 min). Triangles indicate the cleaved fragments on a urea polyacrylamide gel (left). Cleavage sites and generated fragments are mapped on the target RNA sequence (right). Dotted circles represent the region covered by the *ToCsm3* subunit according to previous reports [19,21,22]. The RNA substrate was 5' end-labelled with ^{32}P (yellow asterisk).

B Target RNA-activated DNA cleavage by the wild-type (WT) and mutant *ToCsm* complex. The mutant *ToCsm* complex containing a *ToCsm1* mutant (HD_m , *ToCsm1*^{H14A/D15N}; DD_m , *ToCsm1*^{D587A/D588A}; or HD/DD_m , *ToCsm1*^{H14A/D15N/D587A/D588A}). Target ssDNA substrate (left) and non-target ssDNA substrate (right). "Control" indicates the reaction with wild-type *ToCsm* complex in the absence of target RNA. The arrow on the left panel indicates the largest cleavage product.

Source data are available online for this figure.

the complementary sequence (Fig EV4C). The *ToCsm* complex bound to the target ssDNA and RNA with a dissociation constant (K_D) of approximately 1.5 nM (ssDNA) and 1.3 nM (RNA), respectively (Fig 3A–C). An ssDNA version containing a non-complementary sequence exhibited only a marginal shift at high concentration of the *ToCsm* complex (Fig 3D and E). The *ToCsm* complexes containing the *ToCsm1* (HD_m), *ToCsm1* (DD_m) or *ToCsm1* (HD/DD_m) mutant interacted with the target ssDNA without a notable difference compared with the wild-type *ToCsm* complex,

demonstrating that these mutations in *ToCsm1* do not affect the interaction of the effector complex with the target nucleotide (Fig EV4D). A significantly diminished mobility shift of the target ssDNA was observed by pre-incubation of the *ToCsm* complex with the target RNA. In contrast, pre-incubation of the complex with a non-target RNA did not affect the mobility shift (Fig 3F and G). EMSAs performed in the presence of competing nucleotides indicated that the *ToCsm* complex binds the target ssDNA and RNA, indistinguishably (Fig 3H and I). Together, these data

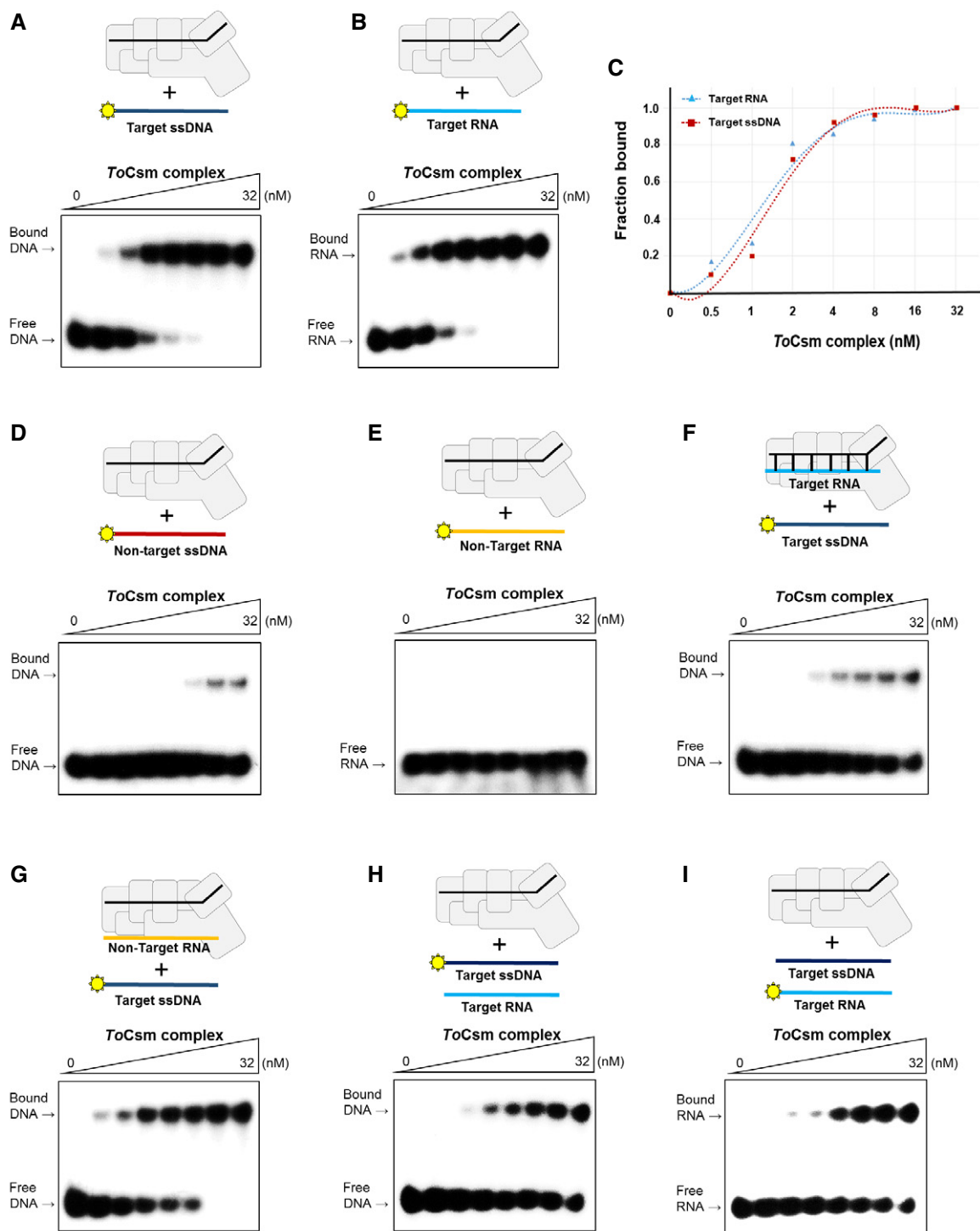


Figure 3. Binding properties of ToCsm complex to target ssDNA and RNA.

A, B EMSA analysis of the interaction between the ToCsm complex and the target ssDNA (A) or the target RNA (B).

C Binding affinity of ToCsm complex for target ssDNA and target RNA. The fraction of target bound to the titrating ToCsm complex in (A) and (B). The K_D value obtained from the curve fitting is indicated. ToCsm complex to target ssDNA $K_D \sim 1.5 \pm 0.37$ nM; ToCsm complex to target RNA $K_D \sim 1.3 \pm 0.32$ nM.

D, E EMSA analysis of the interaction between the ToCsm complex and the non-target ssDNA (D) or the non-target RNA (E).

F, G Interaction between the labelled target ssDNA and the ToCsm complex that was pre-incubated with unlabelled target RNA (F) or unlabelled non-target RNA (G) at a molar ratio of 1:1.

H, I Competition binding of the labelled target ssDNA and the unlabelled target RNA (H) or the unlabelled target ssDNA and the labelled target RNA (I) to the increasing amount of the ToCsm complex.

Source data are available online for this figure.

indicate that the interaction of the *ToCsm* complex with the target ssDNA is mediated by the bound crRNA via complementary base pairing between its guide sequence and the target sequence in the ssDNA.

Target RNA-independent cleavage of ssDNA

To examine whether, in the absence of a target RNA, the *ToCsm* complex can cleave ssDNA, which contains a target sequence, we prepared two different crRNAs: M13 crRNA containing a sequence complementary to the circular M13mp18 ssDNA and 3.3 crRNA containing a non-complementary sequence. The *ToCsm* complex assembled with M13 crRNA or 3.3 crRNA was incubated with M13mp18. The *ToCsm* complex loaded with M13 crRNA completely degraded M13mp18, whereas the effector complex loaded with 3.3 crRNA did not. Under the same reaction conditions, the M13 crRNA-loaded *ToCsm* complex did not degrade Φ X174, a circular ssDNA but with a different sequence (Fig 4A). These data clearly indicate that the *ToCsm* complex possesses a crRNA-guided nuclease activity in the absence of a target RNA. To locate the active site of the *ToCsm* complex responsible for the nuclease activity, we performed cleavage assay with the *ToCsm* complex containing the *ToCsm1* (HD_m), *ToCsm1* (DD_m) or *ToCsm1* (HD/DD_m) mutant. The *ToCsm1* (HD_m)- or *ToCsm1* (HD/DD_m)-containing *ToCsm* complex could not degrade M13mp18, while the effector complex containing *ToCsm1* (DD_m) completely degraded the substrate (Fig 4A). Mn²⁺ or Ni²⁺ supported the nuclease activity, while Mg²⁺ or Ca²⁺ (required for the RNase activity of the *ToCsm3* subunit) did not (Fig 4B). In addition, the effector complex containing *ToCsm3*^{D36A} cleaved the ssDNA substrate without a notable difference from the wild-type complex (Fig 4C). These results demonstrate that the HD domain of the *ToCsm1* subunit is the active site for the target RNA-independent ssDNA cleavage.

Identification of the target RNA-independent ssDNA cleavage sites

To gain further insight into the mechanism of the target ssDNA cleavage in the absence of a target RNA, we synthesized a linear radio-labelled 100-nt ssDNA containing a target sequence in the middle, a 10-nt non-complementary sequence at the 5' end and a 60-nt non-complementary sequence at the 3' end of the DNA. Upon reaction with the *ToCsm* complex assembled with the M13 crRNA, this ssDNA substrate, termed target ssDNA, was cleaved to yield a 52–54-nt fragment (Figs 5A and EV5A). Cleavage occurred at the 3' flanking side of the complementary segment, approximately 12–14 nt downstream from position 1 of the guide region of the crRNA (Fig 5B). The *ToCsm* complex containing *ToCsm1* (HD_m) or *ToCsm1* (HD_m/DD_m) did not show any cleavage activity towards the 5' radio-labelled target ssDNA, whereas the *ToCsm* complex containing *ToCsm1* (DD_m) degraded this substrate (Fig 5C). In contrast, ssDNA substrate containing a non-complementary sequence or dsDNA was not cleaved (Fig EV5B and C). We noted that the same 100-nt ssDNA, but with a 3' radio-labelled, exhibited a near complete degradation, producing 10–25-nt fragments (Fig 5D). The *ToCsm* complex containing *ToCsm3*^{D36A} exhibited the same DNA cleavage pattern as the wild-type effector complex (Fig 5E). These data suggest that the *ToCsm* complex cleaves the target ssDNA

substrate at the 3' side of the complementary sequence and degrades the 3' end fragment.

Suppression of the target RNA-independent ssDNA cleavage by a repeat-derived sequence

The repeat-derived 5' handle of the bound crRNA was reported to play a key role in self versus non-self discrimination in the Type III system-mediated immunity [37]. In a trans-cleavage assay where ssDNA substrates were employed as the substrates for the *StCsm* effector complex loaded with a target RNA, it was shown that the presence of a 3' target sequence-flanking region complementary to the 5' handle of the bound crRNA prevented cleavage of the ssDNA substrates [30]. To investigate whether the 3' flanking region of the target sequence affects the target RNA-independent DNA cleavage activity of the *ToCsm* complex, we employed an ssDNA substrate that contained a 3' flanking sequence complementary to the 5' handle of the bound crRNA. Notably, this ssDNA substrate was not degraded at all by the wild-type *ToCsm* complex as well as the *ToCsm* complexes containing a defective *ToCsm1* mutant (Fig 5F), suggesting that the presence of a 5'-handle-complementary sequence in ssDNA substrates blocks this nuclease activity of the *ToCsm* complex (Fig 5G). We next performed a trans-cleavage assay where the *ToCsm* complex was preloaded with a short 40-nt ssDNA or RNA containing a target sequence that is complementary to the guide sequence of the bound crRNA. These nucleotides shared the same sequence and contained a 5-nt 3' flanking region which is not complementary to the 5' handle of the bound crRNA. Both the *ToCsm* complexes degraded the non-target Φ X174 plasmid DNA (Fig EV5D). It is noted that the *ToCsm* complex containing *ToCsm1* (HD_m) or *ToCsm1* (HD/DD_m) could not degrade Φ X174, while the effector complex containing *ToCsm1* (DD_m) degraded this substrate. Intriguingly, *ToCsm* complex loaded with a target ssDNA or RNA lacking the 3' flanking sequence could not degrade Φ X174 plasmid DNA (Fig EV5E). These data demonstrate that the nuclease activity of the HD domain is activated by nucleotide binding to the *ToCsm* complex, but the bound nucleotide should have a 3' target sequence-flanking segment that does not base pair with the 5' handle of the bound crRNA.

Selective cleavage of partially unwound DNA duplex

Next, we examined whether the *ToCsm* complex could cleave partly unwound DNA duplex containing a target sequence. We prepared an artificial bubble DNA substrate containing 80-nt unwound strands in the centre flanked by 25-nt double-stranded segments at both ends. In this DNA duplex, one strand contained a 30-nt target sequence in the middle of the single-stranded region (target strand), and the other strand (non-target strand) contained an 80-nt sequence not complementary to the target strand. This DNA duplex mimics a “transcription bubble” (Fig EV5F). In order to trace reaction products, two versions of the DNA duplex were prepared that were radio-labelled at the 5' end of either the target strand or the non-target strand. Upon reaction with the *ToCsm* complex, the target strand was cleaved to yield approximately 85-nt long fragments (Fig 6A), while the non-target strand was not cleaved at all (Fig 6B). We also prepared a DNA duplex in which the target strand contained a sequence complementary to both the 5' handle and the

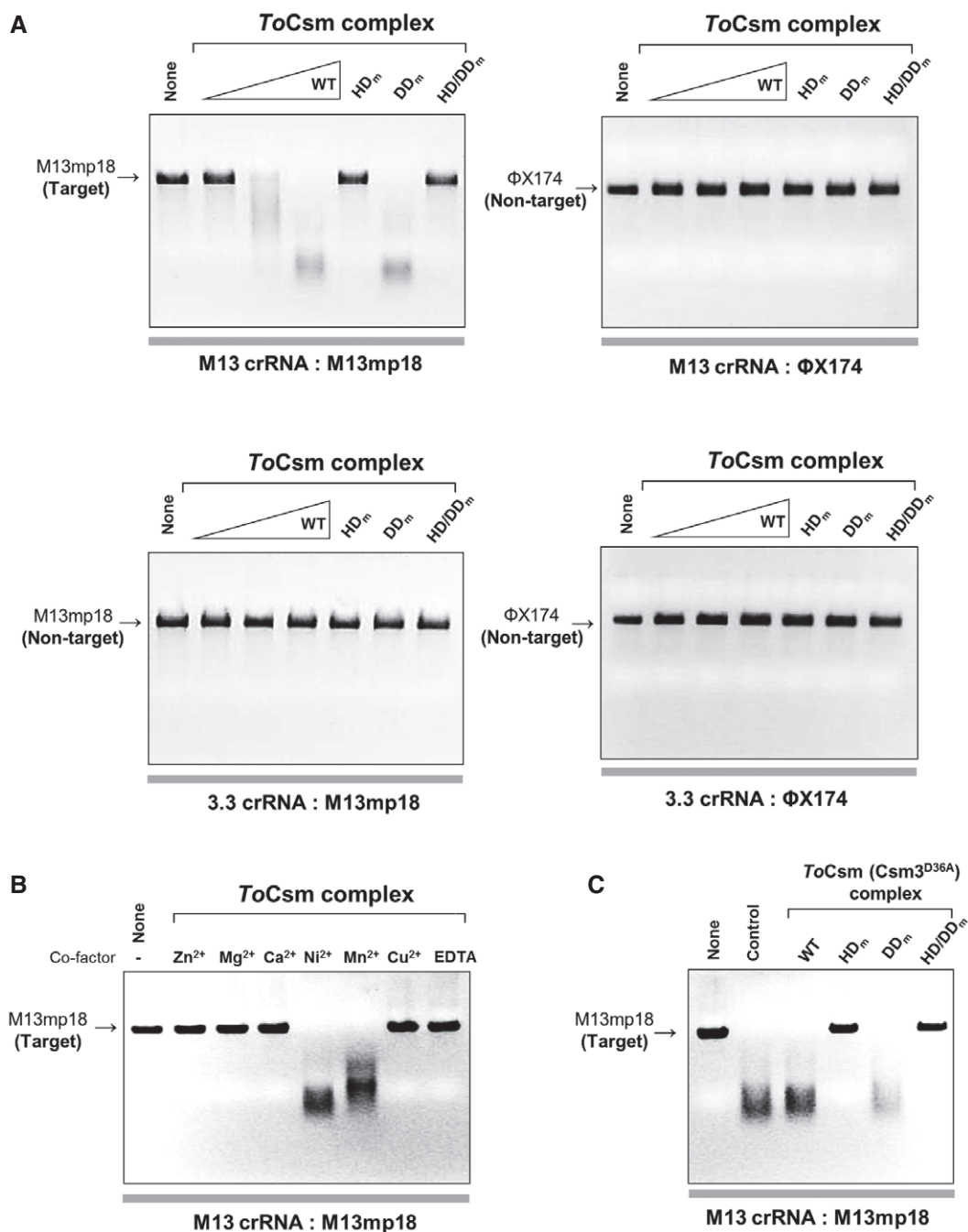


Figure 4. Target RNA-independent cleavage of target ssDNA.

A Cleavage of circular ssDNA by the *ToCsm* complex loaded with the M13 crRNA or 3.3 crRNA. The *ToCsm* complexes containing a *ToCsm1* mutant are indicated as in Fig 2B. M13 crRNA contains a sequence complementary to M13mp18. The crRNA-DNA substrate pairs are indicated at the bottom of the polyacrylamide gel. The *ToCsm* complexes were incubated with the ssDNA substrate in the presence of 5 mM Ni²⁺.

B Metal ion-dependency test. The *ToCsm* complex loaded with M13 crRNA was reacted with M13mp18 ssDNA in the presence of the indicated metal ions.

C Cleavage of circular ssDNA by the *ToCsm* complexes containing *ToCsm3^{D36A}* and wild-type (WT) or mutant *ToCsm1* (HD_m, DD_m or HD/DD_m). "Control" represents the reaction with the wild-type *ToCsm* complex.

Source data are available online for this figure.

guide region of the crRNA and found that the *ToCsm* complex did not cleave the target strand at all (Fig 6C). Conclusively, the *ToCsm* complex is able to selectively cleave the target strand in

partially unwound DNA that exposes the target sequence on this strand in the absence of a target RNA. This nuclease activity, however, was completely blocked by the presence of the 8-nt

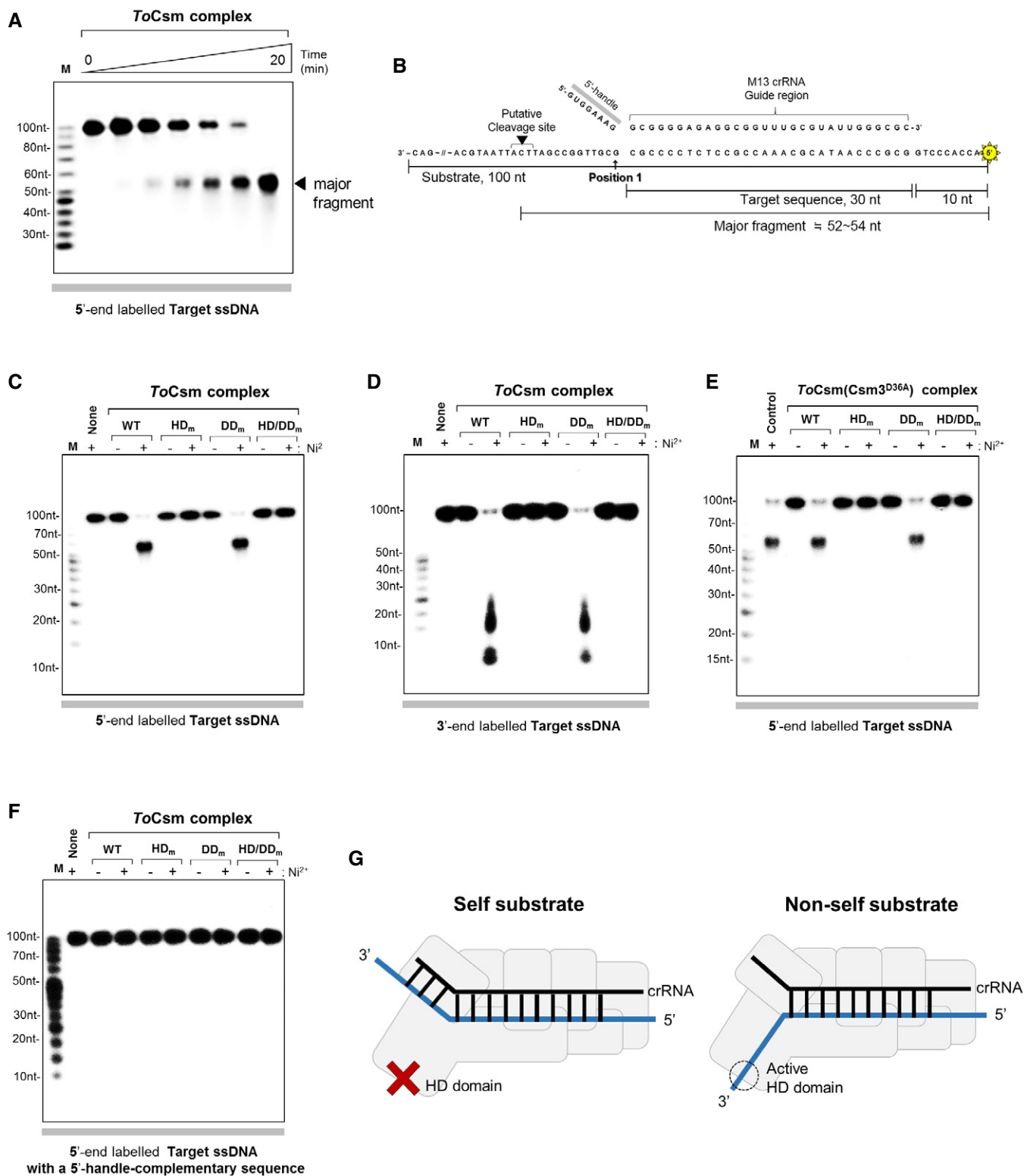


Figure 5.

5'-handle-complementary sequence next to the target sequence. Likely, this inhibitory mechanism prevents the *ToCsm* complex from cleaving self DNA when the CRISPR loci are transcribed [19,37].

Discussion

We reconstituted a *ToCsm* complex, which is conceivably the same as the endogenous functional form, as it possesses the RNase

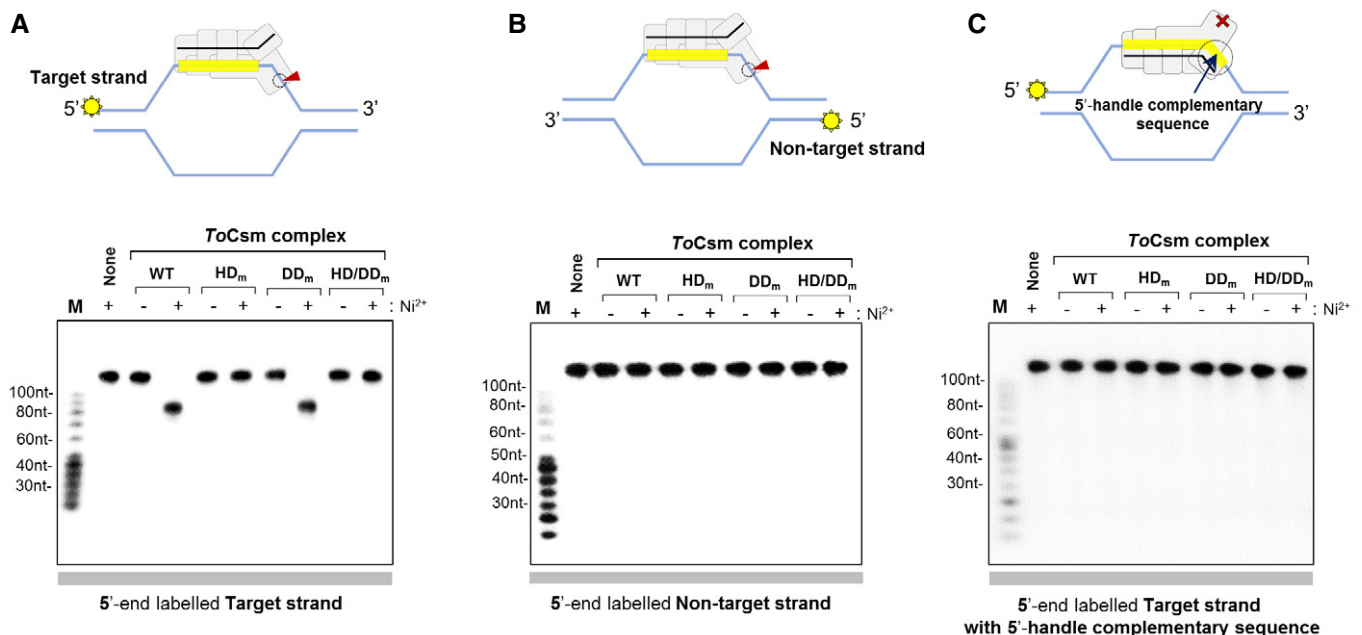
Figure 5. ssDNA targeting mechanism by the *ToCsm* complex.

- A Cleavage of linear target ssDNA by the *ToCsm* complex in a time course (0, 0.5, 1, 3, 5, 10, 20 min). The radio-labelled substrate is indicated at the bottom of the polyacrylamide gel. The triangle indicates the major cleaved fragment.
- B The major fragment is mapped on the sequence of the linear ssDNA substrate. Position 1 denotes the 3' end of the target sequence. 5' radio-labelling (asterisk) and the approximate length of the major fragment are indicated.
- C Cleavage of 5' radio-labelled linear target ssDNA by the wild-type (WT) and mutant *ToCsm* complex. The *ToCsm* complexes containing a *ToCsm1* mutant are indicated as in Fig 2B.
- D Cleavage of 3' radio-labelled linear target ssDNA by the wild-type (WT) and mutant *ToCsm* complex.
- E Cleavage of 5' radio-labelled linear target ssDNA by the *ToCsm* complexes containing *ToCsm3*^{D36A} and wild-type or mutant *ToCsm1*. "Control" represents the reaction with the wild-type *ToCsm* complex.
- F Cleavage of 5' radio-labelled linear target ssDNA containing the 8-nt sequence complementary to the 5' handle of the crRNA.
- G A model for the discrimination of self and non-self ssDNA by the *ToCsm* complex. The non-self substrate ssDNA does not contain a sequence complementary to the 5' handle of the crRNA (right). The putative closed and open states of the active site of the HD domain are indicated by a cross and a dotted circle, respectively.
- Source data are available online for this figure.

activity and the target RNA-activated non-sequence-specific DNase activity observed for other Csm complexes [19,23,30]. This effector complex was found to recognize a target sequence in ssDNA via the bound crRNA and cleave the substrate via the HD domain of the *ToCsm1* subunit in a target RNA-independent manner. Although the activated HD in the *ToCsm* complex upon binding to the 3' flanking sequence of target ssDNA is able to cleave ssDNA substrate in a trans-acting manner (Fig EV5D), the degradation of the target strand in the bubble-shaped DNA duplex indicates a direct *cis*-acting activity of this effector (Fig 6A and B). Given the observation that the Type III-A system of *S. epidermidis* tolerates

lysogenization by temperate phages, but prevents their lytic phase [33], Csm complexes seem to function during transcription. Further investigation is required to know whether the *ToCsm* complex may target ssDNA in the transcription bubble and whether the *cis*-acting activity that we observed in *in vitro* may be functionally relevant in cells.

The novel ssDNA targeting activity of the *ToCsm* complex, which needs further investigation in cells, provides a more complete picture of how transcription is coupled to the destruction of non-self DNA. One effector complex activated by the RNA transcript produced during the transcription process non-specifically

**Figure 6. Cleavage of target ssDNA in DNA duplex.**

- A–C Cleavage of the target strand (A), the non-target strand (B) and the target strand with the 5'-handle-complementary sequence (C) in DNA duplex. The bubble-form DNA duplex (shown in cartoons) was generated by a central non-complementary region in the two DNA strands (see text for details). The indicated *ToCsm* complexes were incubated with the 5' end-labelled duplex DNA, and the reaction products were analysed by autoradiography. The cartoons depict the expected cleavage or non-cleavage of the target strand, depending on the presence or absence of the 5'-handle-complementary sequence. The red arrow indicates the cleavage at the active site of the HD domain of the *ToCsm1* subunit.

Source data are available online for this figure.

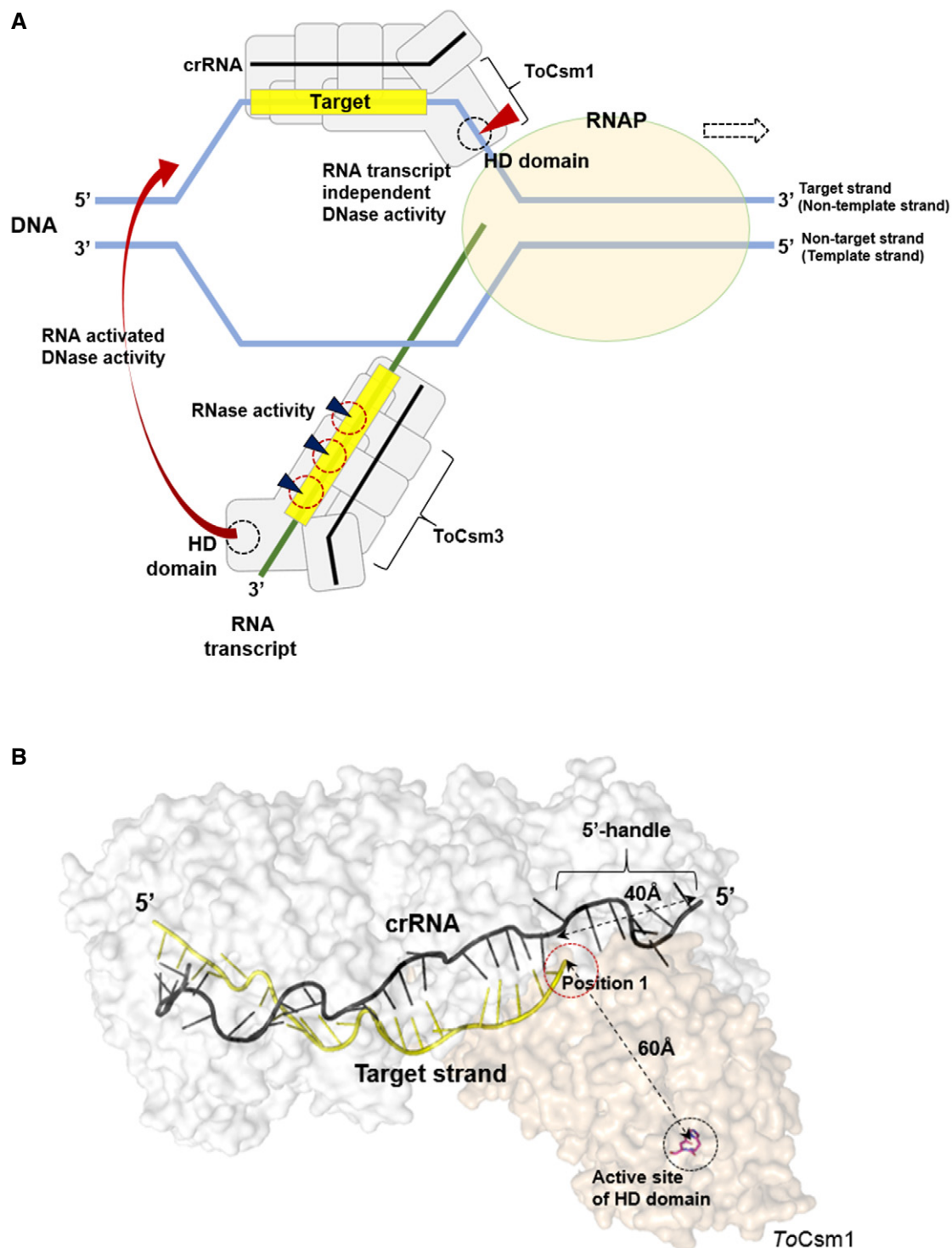


Figure 7. Model for ssDNA targeting by the ToCsm complex.

- A** Transcription-coupled cleavages of foreign dsDNA and RNA by the ToCsm complex. RNAP stands for RNA polymerase. The blue triangle indicates the cleavage of the RNA transcript (green line) by the ToCsm3 subunit. Binding of the RNA transcript to the ToCsm complex activates the DNase activity of the HD domain, which cleaves the template or non-template strands. Another ToCsm complex directly recognizes the exposed target sequence on the non-template strand mediated by the bound crRNA (black line). Without a need for an RNA transcript, the complex cleaves the non-template strand mediated by the ToCsm1 subunit (red triangle).
- B** The structural model of the ToCsm Complex with target ssDNA. The distance between position 1 of the target region and the active site of the HD domain is comparable to the length of nucleotides from the sequence of position 1 to the cleavage site. The ToCsm1 structure (PDB ID: 4UW2, wheat) was modelled to ToCsm complex EM map (EMD-3454) and the Cmr complex structure (PDB ID: 3X1L, white) based on the position of Cmr2 to highlight the active site of the HD domain.

cleaves any exposed DNA strands of the transcription bubble, and another effector complex activated by binding to the target sequence on the non-template strand may cleave this strand directly (Fig 7A) [41]. The destruction of the foreign DNA by target RNA-activated ssDNase mechanism may not be sufficient alone; during the transcription of foreign DNA, the Type III effector complex, which cleaves ssRNA faster than it cleaves ssDNA [30], may dissociate from the tethering RNA transcript without cleaving the single-stranded region of the transcription bubble. Notably, the delineated target RNA-independent ssDNA cleavage could explain previously reported observations. First, this activity, which exclusively targets the non-template DNA strand of DNA duplex, in contrast with the non-discriminative target RNA-activated ssDNase activity, explains why crRNA complementary to the non-template DNA provides efficient immunity and why a spacer sequence on the non-template strand is preferentially selected for cleavage during transcription [19,33]. Second, the location of the HD domain relative to the target sequence binding site on the *ToCsm* complex explains the previously identified cleavage sites on the non-template DNA strand located at the 3' side of the guide region of the bound crRNA (Fig 7B) [19]. By the RNA transcript-dependent ssDNAase activity, the non-template strand, in principle, could be cleaved at random positions with respect to the target sequence on it. However, it was observed that the non-template strand cleavage mediated by the Type III-A system of *S. epidermis* occurs only at the 3' flanking side of the target sequence [19], which is consistent with the pattern of cleavage by the target RNA-independent ssDNase activity observed in this study. Finally, the blocking of this nuclease activity by the presence of the 5'-handle-complementary sequence next to the target sequence provides a rationale for the previously observed protection of self DNA from cleavage by the Type III system [19,37]. The RNA transcript-independent cleavage of target ssDNA by the *ToCsm* complex may be pivotal, or at least it could augment the previously known target RNA-activated DNase activity for the efficient destruction of foreign DNA molecules in cells. Alternatively, the *ToCsm* complex could play a specific role against ssDNA viruses, rather than acting on genomic dsDNA. Recently, some Cas9s were reported to bind to ssDNA with higher affinity than to dsDNA, demonstrating a significant divergence of the CRISPR-Cas systems [42].

In summary, we reconstituted a highly pure and functionally active Type III effector complex, the smallest Csm complex observed so far with a minimum combination of subunits. Type I, II and III systems may share a common mechanism of crRNA-mediated target DNA sequence recognition, although the mechanisms of target cleavage are different from each other. The RNA activation-independent ssDNA targeting activity highlights the versatility of the Type III effector complex in *T. onnurineus* for the efficient and complete silencing of foreign nucleic acids.

Materials and Methods

Cloning and protein purification

The genes encoding *ToCsm1*–*ToCsm5* (Ton_0893–0897) were amplified by PCR from *T. onnurineus* NA1 genomic DNA. The *ToCsm1*

and *ToCsm4* genes were cloned into the BamHI/HindIII and the NdeI/KpnI sites of the pRSFDuet-1 vector (Novagen), respectively. The *ToCsm3* gene was inserted into the NcoI/SalI sites of pETDuet-1 (Novagen), and the *ToCsm2*–*ToCsm5* genes were inserted into the NcoI/SalI and the NdeI/XhoI sites of pACYCDuet-1 (Novagen). These Csm proteins were produced in the *E. coli* strain BL21-Codon-Plus (DE3) at 37°C by induction with 1 mM IPTG. *E. coli* cells were harvested and lysed. Following centrifugation, the supernatant was incubated in a hot water bath at 75°C for 10 min to remove *E. coli* proteins. After clarification, the supernatant was applied to a His-Trap HP column (GE Healthcare) and a Superdex 200 increase 10/300 column (GE Healthcare) with a final elution buffer composed of 50 mM Tris–HCl (pH 8.0), 500 mM NaCl, 5 mM β -mercaptoethanol and 5% glycerol.

In vitro assembly of the ToCsm complex and SEC-MALS

Synthetic crRNAs were purchased from Integrated DNA Technologies. After initial optimization, the purified *ToCsm1*–*Csm4*, *ToCsm3*, *ToCsm2*–*Csm5* and crRNA were mixed in a molar ratio of 1:3:1:1 and then incubated at 60°C for 20 min. After centrifugation at 10,000 g for 5 min, the protein sample was applied to a Superdex 200 increase 10/300 column (GE Healthcare) and equilibrated with 50 mM Tris–HCl (pH 8.0), 250 mM NaCl and 5% glycerol. Fractions containing the *ToCsm* complex were pooled and applied again to the Superdex 200 increase 10/300 column. The assembled samples and the size marker (GenDEPOT, Novex and Affymetrix) were analysed on 15% SDS gel, 4–12% BN–PAGE gel and 12% polyacrylamide denaturing 8 M urea gels. SEC–MALS was performed using a WTC-050S5 SEC column with an in-line DAWN HELIOS II system and an Optilab T-rEX differential refractometer (Wyatt). The *ToCsm* complex (100 μ l of 1 mg/ml) was dissolved in a buffer solution composed of 50 mM Tris–HCl (pH 8.0), 250 mM NaCl, 3 mM β -mercaptoethanol. Data were collected and analysed using ASTRA 6 (Wyatt). The *ToCsm* complexes containing a mutant Csm1 subunit were reconstituted and purified in the same manner as the wild-type *ToCsm* complex. The purified complex was frozen in liquid nitrogen and stored at –80°C.

Site-directed mutagenesis of ToCsm1 and ToCsm3

The *ToCsm1* mutants (HD_m, *ToCsm1*^{H14A/D15N}; DD_m, *ToCsm1*^{D587A/D588A}; and HD/DD_m, *ToCsm1*^{H14A/D15N/D587A/D588A}) and the *ToCsm3* mutant (*ToCsm3*^{D36A}) were generated with the site-directed mutagenesis kit (Enzymonics). The mutations were verified by sequencing the respective genes (Solgent).

Electron microscopy

The *ToCsm* complex was negatively stained with 2% (w/v) uranyl acetate for 1 min on 400-mesh carbon grids. Images were collected at a magnification of 50,000 \times at a final sampling of 2.07 Å/pixel with a defocus value of 0.5–1.5 μ m on a 4 \times 4 K CCD camera (Tietz Vio and imaging Processing System) attached to Jeol JEM2100F field emission gun transmission electron microscope operated at 200 kV. Data processing was performed using the EMAN2 program [43]. In total, 7,644 particles were selected and used to generate reference-free 2D class averages. The initial model was built from

34 selected classes using the `e2initialmodel.py` program. Then, the model was further iteratively refined by the `e2refine_easy.py` program with a low-pass filter (cut-off = 0.04). The resolution was estimated as 25 Å from the last iteration of the unmasked 0.5 FSC curve. The 3D map of *ToCsm* has been deposited in the PDB; EMD-3454. The crystal structure of Cmr complex (PDB ID: 3X1L) into the refined 3D map of *ToCsm* (EMD-3454) was docked by the “Fit in map” function of Chimera software [44].

Preparation of substrates

The RNA and DNA substrates were purchased from Integrated DNA Technologies and Bioneer, respectively (Table EV1). The DNA and the RNA substrates were 5'-labelled with γ P³²-ATP (Perkin Elmer) and T4 PNK enzyme (Enzymomics) at 37°C for 20 min, respectively. DNA substrates were 3'-labelled with α P³²-dATP (Perkin Elmer) and TDT enzyme (Enzymomics) for 40 min at 37°C. Circular ssDNA of M13mp18 and Φ X174 Virion was purchased (New England BioLabs). To generate the bubble shape DNA, each oligonucleotide was mixed at a 1:1 molar ratio in reaction buffer (50 mM Tris-HCl pH 8.0, 50 mM NaCl₂), heated to 95°C for 5 min and slowly cooled to room temperature for annealing.

Electrophoretic mobility shift assay

DNA/RNA binding assays were performed by incubating varying amounts (0, 0.5, 1, 2, 4, 8, 16, 32 nM) of the *ToCsm* complexes at 55°C for 20 min with 1 nM γ P³²-ATP and 5'-labelled 40-nt DNA and/or 40-nt RNA in binding buffer composed of 30 mM Tris-HCl (pH 8.0), 5% glycerol, 0.1 mg/ml BSA and 0.5 mM EDTA. The samples were loaded directly onto native 8% (w/v) polyacrylamide gel. Electrophoresis was carried out at room temperature at 100 V for 80 min using running buffer composed of 0.5× TBE and 0.1 mM EDTA. Gels were dried and visualized using an FLA-5100 phosphorimager (Fujifilm). The K_D of the ssDNA and RNA binding of the *ToCsm* complex was evaluated assuming the complex concentration at which half of the substrate is bound as a rough estimate of K_D value.

RNA cleavage assay

The *ToCsm* complex (600 nM) and the radio-labelled RNA substrate (2 nM) were incubated at 55°C for 5 min in reaction buffer A composed of 30 mM Tris-HCl (pH 8.0), 100 mM KCl, 100 mM NaCl and 3% glycerol. The reactions were initiated by the addition of 5 mM MnCl₂ and incubated at 55°C for 20 min. The reactions were stopped by the addition of formamide loading buffer B composed of 95% formamide, 0.025% SDS, 0.01% bromophenol blue, 0.01% xylene cyanol and 1 mM EDTA, followed by heating at 95°C for 10 min. The samples and the size marker (Affymetrix) were analysed on 12.5% polyacrylamide denaturing 8 M urea gels and visualized by phosphorimaging (Fujifilm).

Target RNA-dependent DNA cleavage assay

The *ToCsm* complex (600 nM) and the unlabelled 40-nt target RNA (600 nM) were incubated at 55°C for 15 min in reaction buffer A with 5 mM NiSO₄. The reaction was initiated by the addition of

radio-labelled 100-nt DNA (2 nM) and incubated at 55°C for 20 min. The reaction was stopped by the addition of sample loading buffer B followed by heating at 95°C for 10 min. The samples and the size marker (Affymetrix) were analysed on 10% polyacrylamide denaturing 8 M urea gels and visualized by phosphorimaging (Fujifilm).

Target RNA-independent DNA cleavage assay

Reactions with the *ToCsm* complex (30 nM) and the circular single-stranded DNA substrates (5 nM) M13mp18 or Φ X174 were carried out in buffer A with 5 mM NiSO₄. After incubation at 55°C for 20 min, the reactions were quenched by the addition of 6× DNA loading dye (Fermentas) and analysed on 1% agarose gels. For the radio-labelled linear DNA substrates (2 nM), reactions were carried out with the *ToCsm* complex (600 nM) and stopped by the addition of formamide loading buffer B and heating at 95°C for 10 min. The samples and the size marker (Affymetrix) were analysed by 10% polyacrylamide denaturing 8 M urea gels and visualized by phosphorimaging (Fujifilm).

Trans-ssDNA cleavage assay

The *ToCsm* complex (30 nM) and the unlabelled target ssDNA (30 nM) or target RNA (30 nM) were incubated at 55°C for 15 min in reaction buffer A with 5 mM NiSO₄. The reaction was initiated by the addition of circular single-stranded DNA substrates Φ X174 (5 nM), incubated at 55°C for 20 min and quenched by the addition of 6× DNA loading dye (Fermentas) before analysis on 1% agarose gels.

Expanded View for this article is available online.

Acknowledgements

We thank Dr. Kang Sung-Gyun in KIOST for providing the genomic DNA of *T. onnurineus* NA1. This work was partly supported by the Marine and Extreme Genome Research Center programme from the Ministry of Land, Transport and Maritime Affairs and partly by the National Research Foundation of Korea (Grant Number: NRF-2014K1A3A1A49069194/NRF-2015R1A2A2A03006970) and KRIBB Research Initiative Programme. J.-J.S. and H.H. were supported by a STINT-NRF special exchange grant (2014K2A3A1000137). T.-Y.J. is a recipient of a postdoc fellowship from KAIST Institute.

Author contributions

K-HP, B-HO and E-JW conceived the idea. J-HK provided scientific suggestions. K-HP and YA performed protein purification and *In vitro* complex assembly. K-HP, I-YB, W-CA, HN and YA performed experiments. EM work was carried out and analysed by T-YJ, HH and J-JS. The manuscript was written by K-HP, B-HO and E-JW.

Conflict of interest

The authors declare that they have no conflict of interest.

References

- van der Oost J, Westra ER, Jackson RN, Wiedenheft B (2014) Unravelling the structural and mechanistic basis of CRISPR-Cas systems. *Nat Rev Microbiol* 12: 479–492

2. Barrangou R, Fremaux C, Deveau H, Richards M, Boyaval P, Moineau S, Romero DA, Horvath P (2007) CRISPR provides acquired resistance against viruses in prokaryotes. *Science* 315: 1709–1712
3. Marraffini LA, Sontheimer EJ (2008) CRISPR interference limits horizontal gene transfer in staphylococci by targeting DNA. *Science* 322: 1843–1845
4. Bolotin A, Quinquis B, Sorokin A, Ehrlich SD (2005) Clustered regularly interspaced short palindrome repeats (CRISPRs) have spacers of extra-chromosomal origin. *Microbiology* 151: 2551–2561
5. Terns MP, Terns RM (2011) CRISPR-based adaptive immune systems. *Curr Opin Microbiol* 14: 321–327
6. Brouns SJ, Jore MM, Lundgren M, Westra ER, Slijkhuis RJ, Snijders AP, Dickman MJ, Makarova KS, Koonin EV, van der Oost J (2008) Small CRISPR RNAs guide antiviral defense in prokaryotes. *Science* 321: 960–964
7. Mohanraju P, Makarova KS, Zetsche B, Zhang F, Koonin EV, van der Oost J (2016) Diverse evolutionary roots and mechanistic variations of the CRISPR-Cas systems. *Science* 353: aad5147
8. Sinkunas T, Gasiunas G, Fremaux C, Barrangou R, Horvath P, Siksnys V (2011) Cas3 is a single-stranded DNA nuclease and ATP-dependent helicase in the CRISPR/Cas immune system. *EMBO J* 30: 1335–1342
9. Westra ER, van Erp PB, Kunne T, Wong SP, Staals RH, Seegers CL, Bollen S, Jore MM, Semenova E, Severinov K et al (2012) CRISPR immunity relies on the consecutive binding and degradation of negatively supercoiled invader DNA by Cascade and Cas3. *Mol Cell* 46: 595–605
10. Gasiunas G, Barrangou R, Horvath P, Siksnys V (2012) Cas9-crRNA ribonucleoprotein complex mediates specific DNA cleavage for adaptive immunity in bacteria. *Proc Natl Acad Sci USA* 109: E2579–E2586
11. Garneau JE, Dupuis ME, Villion M, Romero DA, Barrangou R, Boyaval P, Fremaux C, Horvath P, Magadan AH, Moineau S (2010) The CRISPR/Cas bacterial immune system cleaves bacteriophage and plasmid DNA. *Nature* 468: 67–71
12. Fonfara I, Richter H, Bratovic M, Le Rhun A, Charpentier E (2016) The CRISPR-associated DNA-cleaving enzyme Cpf1 also processes precursor CRISPR RNA. *Nature* 532: 517–521
13. Makarova KS, Haft DH, Barrangou R, Brouns SJ, Charpentier E, Horvath P, Moineau S, Mojica FJ, Wolf YI, Yakunin AF et al (2011) Evolution and classification of the CRISPR-Cas systems. *Nat Rev Microbiol* 9: 467–477
14. Makarova KS, Wolf YI, Alkhnbashi OS, Costa F, Shah SA, Saunders SJ, Barrangou R, Brouns SJ, Charpentier E, Haft DH et al (2015) An updated evolutionary classification of CRISPR-Cas systems. *Nat Rev Microbiol* 13: 722–736
15. Jore MM, Lundgren M, van Duijn E, Bultema JB, Westra ER, Waghmare SP, Wiedenheft B, Pul U, Wurm R, Wagner R et al (2011) Structural basis for CRISPR RNA-guided DNA recognition by Cascade. *Nat Struct Mol Biol* 18: 529–536
16. Rouillon C, Zhou M, Zhang J, Politis A, Beilsten-Edmands V, Cannone G, Graham S, Robinson CV, Spagnolo L, White MF (2013) Structure of the CRISPR interference complex CSM reveals key similarities with cascade. *Mol Cell* 52: 124–134
17. Hatoum-Aslan A, Maniv I, Samai P, Marraffini LA (2014) Genetic characterization of antiplasmid immunity through a type III-A CRISPR-Cas system. *J Bacteriol* 196: 310–317
18. Peng W, Feng M, Feng X, Liang YX, She Q (2015) An archaeal CRISPR type III-B system exhibiting distinctive RNA targeting features and mediating dual RNA and DNA interference. *Nucleic Acids Res* 43: 406–417
19. Samai P, Pyenson N, Jiang W, Goldberg GW, Hatoum-Aslan A, Marraffini LA (2015) Co-transcriptional DNA and RNA Cleavage during Type III CRISPR-Cas Immunity. *Cell* 161: 1164–1174
20. Hale CR, Zhao P, Olson S, Duff MO, Graveley BR, Wells L, Terns RM, Terns MP (2009) RNA-guided RNA cleavage by a CRISPR RNA-Cas protein complex. *Cell* 139: 945–956
21. Tamulaitis G, Kazlauskienė M, Manakova E, Venclovas C, Nwokeoji AO, Dickman MJ, Horvath P, Siksnys V (2014) Programmable RNA shredding by the type III-A CRISPR-Cas system of *Streptococcus thermophilus*. *Mol Cell* 56: 506–517
22. Staals RH, Zhu Y, Taylor DW, Kornfeld JE, Sharma K, Barendregt A, Koehorst JJ, Vlot M, Neupane N, Varossieau K et al (2014) RNA targeting by the type III-A CRISPR-Cas Csm complex of *Thermus thermophilus*. *Mol Cell* 56: 518–530
23. Zhang J, Graham S, Tello A, Liu H, White MF (2016) Multiple nucleic acid cleavage modes in divergent type III CRISPR systems. *Nucleic Acids Res* 44: 1789–1799
24. Cao L, Gao CH, Zhu J, Zhao L, Wu Q, Li M, Sun B (2016) Identification and functional study of type III-A CRISPR-Cas systems in clinical isolates of *Staphylococcus aureus*. *Int J Med Microbiol* 306: 686–696
25. Hale CR, Coczaki A, Li H, Terns RM, Terns MP (2014) Target RNA capture and cleavage by the Cmr type III-B CRISPR-Cas effector complex. *Genes Dev* 28: 2432–2443
26. Zhang J, Rouillon C, Kerou M, Reeks J, Brugger K, Graham S, Reimann J, Cannone G, Liu H, Albers SV et al (2012) Structure and mechanism of the CMR complex for CRISPR-mediated antiviral immunity. *Mol Cell* 45: 303–313
27. Carte J, Wang R, Li H, Terns RM, Terns MP (2008) Cas6 is an endoribonuclease that generates guide RNAs for invader defense in prokaryotes. *Genes Dev* 22: 3489–3496
28. Osawa T, Inanaga H, Sato C, Numata T (2015) Crystal structure of the CRISPR-Cas RNA silencing Cmr complex bound to a target analog. *Mol Cell* 58: 418–430
29. Benda C, Ebert J, Scheltema RA, Schiller HB, Baumgartner M, Bonneau F, Mann M, Conti E (2014) Structural model of a CRISPR RNA-silencing complex reveals the RNA-target cleavage activity in Cmr4. *Mol Cell* 56: 43–54
30. Kazlauskienė M, Tamulaitis G, Kostiuk G, Venclovas C, Siksnys V (2016) Spatiotemporal control of type III-A CRISPR-Cas immunity: coupling DNA degradation with the target RNA recognition. *Mol Cell* 62: 295–306
31. Estrella MA, Kuo FT, Bailey S (2016) RNA-activated DNA cleavage by the Type III-B CRISPR-Cas effector complex. *Genes Dev* 30: 460–470
32. Elmore JR, Sheppard NF, Ramia N, Deighan T, Li H, Terns RM, Terns MP (2016) Bipartite recognition of target RNAs activates DNA cleavage by the Type III-B CRISPR-Cas system. *Genes Dev* 30: 447–459
33. Goldberg GW, Jiang W, Bikard D, Marraffini LA (2014) Conditional tolerance of temperate phages via transcription-dependent CRISPR-Cas targeting. *Nature* 514: 633–637
34. Hayes RP, Xiao Y, Ding F, van Erp PB, Rajashankar K, Bailey S, Wiedenheft B, Ke A (2016) Structural basis for promiscuous PAM recognition in type I-E Cascade from *E. coli*. *Nature* 530: 499–503
35. Heler R, Samai P, Modell JW, Weiner C, Goldberg GW, Bikard D, Marraffini LA (2015) Cas9 specifies functional viral targets during CRISPR-Cas adaptation. *Nature* 519: 199–202
36. O'Connell MR, Oakes BL, Sternberg SH, East-Seletsky A, Kaplan M, Doudna JA (2014) Programmable RNA recognition and cleavage by CRISPR/Cas9. *Nature* 516: 263–266
37. Marraffini LA, Sontheimer EJ (2010) Self versus non-self discrimination during CRISPR RNA-directed immunity. *Nature* 463: 568–571

38. Jung TY, Park KH, An Y, Schulga A, Deyev S, Jung JH, Woo EJ (2016) Structural features of Cas2 from *Thermococcus onnurineus* in CRISPR-cas system type IV. *Protein Sci* 25: 1890–1897
39. Grissa I, Vergnaud G, Pourcel C (2007) The CRISPRdb database and tools to display CRISPRs and to generate dictionaries of spacers and repeats. *BMC Bioinformatics* 8: 172
40. Jung TY, An Y, Park KH, Lee MH, Oh BH, Woo E (2015) Crystal structure of the Csm1 subunit of the Csm complex and its single-stranded DNA-specific nuclease activity. *Structure* 23: 782–790
41. Barnes CO, Calero M, Malik I, Graham BW, Spahr H, Lin G, Cohen AE, Brown IS, Zhang Q, Pullara F et al (2015) Crystal structure of a transcribing RNA polymerase II complex reveals a complete transcription bubble. *Mol Cell* 59: 258–269
42. Ma E, Harrington LB, O'Connell MR, Zhou K, Doudna JA (2015) Single-stranded DNA cleavage by divergent CRISPR-Cas9 enzymes. *Mol Cell* 60: 398–407
43. Tang G, Peng L, Baldwin PR, Mann DS, Jiang W, Rees I, Ludtke SJ (2007) EMAN2: an extensible image processing suite for electron microscopy. *J Struct Biol* 157: 38–46
44. Pettersen EF, Goddard TD, Huang CC, Couch GS, Greenblatt DM, Meng EC, Ferrin TE (2004) UCSF Chimera—a visualization system for exploratory research and analysis. *J Comput Chem* 25: 1605–1612